ENHANCED SYNERGIC IDENTIFICATION OF PRESTRESS FORCE AND MOVING FORCE IN PRESTRESSED CONCRETE BRIDGES

KUNARATNAM JEYAMOHAN
Ph.D. Student,
School of Civil and Environmental Engineering, Queensland University of Technology (QUT), Brisbane, 4000, Australia

TOMMY.H.T. CHAN
Professor,
School of Civil and Environmental Engineering, Queensland University of Technology (QUT), Brisbane, 4000, Australia

KHAC-DUY NGUYEN
DECRA Postdoctoral Research Follow,
School of Civil and Environmental Engineering, Queensland University of Technology (QUT), Brisbane, 4000, Australia

DAVID P THAMBIRATNAM
Professor
School of Civil and Environmental Engineering, Queensland University of Technology (QUT), Brisbane, 4000, Australia.

Abstract

The estimation and monitoring of the in-service load carrying capacity of prestressed concrete bridge (PCB) structures hold significant importance, especially due to prestress losses occurring with their aging. Therefore, it becomes crucial to develop an effective methodology that requires fewer measurements, enabling the estimation of existing prestress force (PF) and moving force (MF) without relying on detailed knowledge of vehicle characteristics and the prestress bridge-vehicle interaction system. This study proposes an improved methodology for identifying PF and MF synergistically. This approach incorporates displacement measurements and integrates a load shape function (LSF) approach alongside the virtual distortion method. The identification process is improved by adopting a truncation coefficient for LSF, which eliminates ineffective elements and enhances reliability. The proposed improvement technique demonstrates commendable accuracy and facilitates timely maintenance of PCBs. As a result of adopting this approach, engineers and practitioners can assess and monitor the load carrying capacity of PCBs. Consequently, these essential transportation infrastructures can be ensured to be safe and durable for the foreseeable future.

Keywords: Prestressed Concrete Bridges, Moving Force Identification, Prestress Force Identification, Load Shape Function, Truncated Load Shape Function, Load Carrying Capacity

1. Introduction

In recent years, the monitoring of existing prestress force (PF) and the identification of moving force (MF) have gained significant popularity, primarily because of the catastrophic failures of bridge structures around the world. The main intention of these efforts was to estimate the in-service load carrying capacity of prestressed concrete bridges (PCBs).

Numerous researchers have investigated the identification of PF using modal information, including natural frequencies and mode shapes. There is, however, one major challenge associated with this method, which is the inability to detect any significant changes in natural frequency or mode shape because of prestress loss. Also, the modal parameters of PCBs are greatly affected by the effects of strengthening and compressing, which further complicate the analysis (Gan et al., 2019; Law & Lu, 2005; Saiidi et al., 1994). In addition, optical fibre sensors have been used in studies to estimate prestress forces (Gao et al., 2006; Xuan et al., 2009). It is, however, practically impossible to apply this method to existing structures. Further, the accuracy of the results obtained through optical fibre sensors is uncertain due to potential issues such as misalignment, mechanical damage, and improper handling (Gao et al., 2006; Xuan et al., 2009).

A direct measurement of vehicle excitation forces presents significant challenges in terms of cost and complexity, making it virtually impossible to instrument each axle. It is also necessary to consider the mechanism of interaction between the vehicle and the bridge when identifying MFs. As a result, researchers are beginning to focus their efforts on indirect methods of measuring MFs, such as the use of displacements, accelerations, and bending moments. Indirect methods for identifying MFs can be divided into two main categories: analytical methods and numerical methods. Analytical models include time domain analysis (Law et al., 1997), frequency-time domain analysis (Law et al., 1999), and influence line analysis (Yang et al., 2021), while numerical models include interpretive methods-I (IM-I) (Chan et al., 2001), interpretive methods-II (IM-II) (Chan et al., 1999), optimal state estimation approaches (Law & Fang, 2001), and updated static component methods. The choice of method for identifying MFs is greatly influenced by factors such as sensor types, sensor location, number of sensors, and sampling frequency. Furthermore, previous studies primarily concentrated on the analysis of simply supported PCBs.

Furthermore, the identification of PF and MF in a PCB can be accomplished through a load shape function (LSF) approach, which integrates the virtual distortion method and Duhamel integral. This method involves measuring dynamic responses, such as displacements and strains (Xiang et al., 2017; Xiang et al., 2016).

Hence, the identification of PF and MF ultimately becomes an inverse problem characterized by a system of linear algebraic equations. As a result, this force identification process is inherently ill-conditioned. The ill-posed nature of the problem may be mitigated by using various regularization techniques, including truncated generalized singular value decomposition (Chen & Chan, 2017), and modified preconditioned conjugate gradient methods (Chen et al., 2020).

A synchronized assessment method for determining structural damage and MF, and a truncated load shape function (TLSF) were adopted to improve the efficiency and stability of the inverse problem calculation by smoothening pulse function via limited number of TLSF. The proposed

method was also validated for a range of loads and speeds to ensure its robustness and efficiency (Zhong et al., 2022).

Consequently, the primary objective of this study is to improve the accuracy of identifying PF and MF in PCBs. An improved load shape function with a truncating coefficient is proposed to improve force identification accuracy.

2. PF and MF Identification via Load Shape Function Approach

The general equation governing the dynamics of a prestressed bridge vehicle system can be expressed as follows, considering both the effects of MF ($\mathbf{F}(\boldsymbol{t})$) and PF ($\mathbf{T}$).

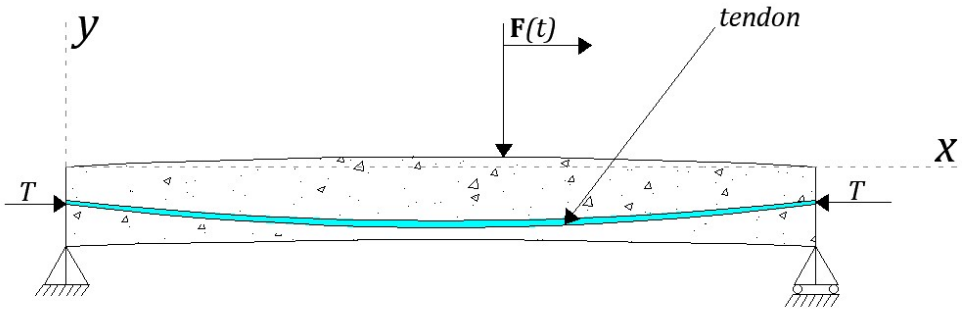

Figure 1 – Prestressed concrete bridge model

$$\mathbf{M}\ddot{\boldsymbol{x}} + \mathbf{C}\dot{\boldsymbol{x}} + \mathbf{K}\boldsymbol{x} = \mathbf{Z}\{\mathbf{F}(t)\} + \mathbf{P} \tag{1}$$

In the above equation. $\boldsymbol{x}$, $\dot{\boldsymbol{x}}$ and $\ddot{\boldsymbol{x}}$ are the displacement, velocity and acceleration vectors respectively; $\mathbf{M}$, $\mathbf{C}$ and $\mathbf{K}$ are the mass, damping and global stiffness of the original structure matrices of the PCB structure, respectively and $\mathbf{Z}$ represents the mapping matrix. As a result of incorporating the Duhamel principle, the dynamic equation can be formulated as follows (Xiang et al., 2017).

$$\mathbf{Y}_j = \mathbf{H}^j\mathbf{F} + \sum_k \sum_i^n \mathbf{D}_{ik}^j \mathbf{P}_{ik} \qquad j = 1, 2, 3, \ldots\ldots nk + 1 \tag{2}$$

where $\mathbf{Y}_j$ is the measured discrete response by the j^{th} sensor while $\mathbf{F}$ and $\mathbf{P}_{ik}$ are the discrete excitation load and virtual force vector respectively. $\mathbf{H}^j$ and $\mathbf{D}_{ik}$ are impulse response matrix and dynamic response matrix of the system composed of impulse response functions between the j^{th} sensor with $\mathbf{F}$ and $\mathbf{P}_{ik}$ respectively.

LSF plays an important role in addressing the identification problem of unknown forces by reducing the unknown parameters and converting them into fitting coefficients. It is possible to develop LSF by considering the vertical displacement as well as rotation of the time-history nodes in the beam.

An approach based on LSF fitting is used to solve inverse problems with a high level of accuracy. In this method, LSF matrix of beam ($\mathbf{N}$) is introduced with the appropriate coefficient ($\boldsymbol{\alpha}$) to replace the unknown load and can be rewritten as shown below.

$$\mathbf{F} = \mathbf{N}\boldsymbol{\alpha} \tag{3}$$

Consequently, the dynamic equation can be extended by incorporating LSF as demonstrated in Equation (4).

$$\mathbf{Y}_j = \mathbf{H}^j \mathbf{N}\boldsymbol{\alpha}_F + \sum_k \sum_i^n \mathbf{D}_{ik}^j \mathbf{N}\boldsymbol{\alpha}_{ik} \qquad j = 1, 2, 3, \ldots\ldots nk + 1 \tag{4}$$

where, $\boldsymbol{\alpha}_F$ and $\boldsymbol{\alpha}_{ik}$ are the relevant coefficient of the moving excitation and coefficient of the k^{th} virtual force caused by i^{th} local pseudo-load. The detailed methodology for identifying the PF and MF based on the LSF approach is illustrated in Figure. 2.

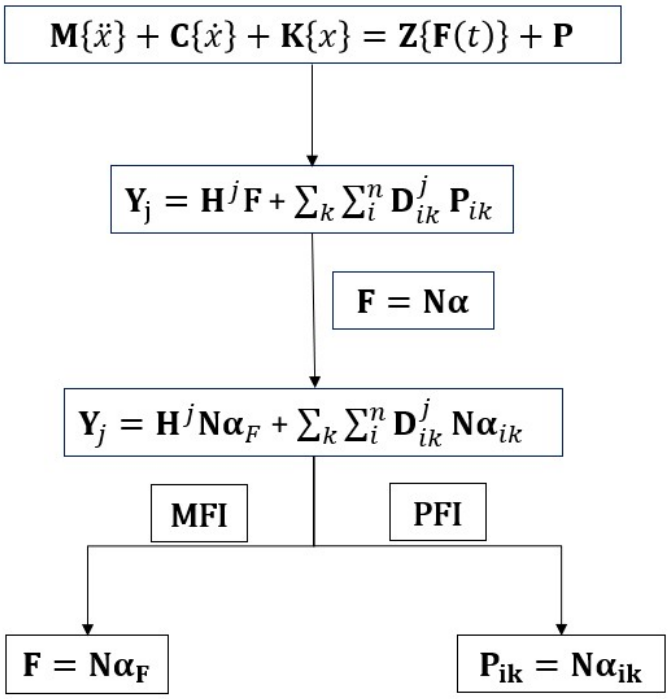

Figure 2- Methodology for LSF based PF and MF identification.

The prestressed beam can be considered as a 2D beam element with axial distortion, bending distortion and bending plus shear distortion to develop the global stiffness matrix ($\mathbf{K}_{g,i}$) of the element considering the PFs as virtual pseudo loads using the virtual distortion method. A bridge structure can be viewed as a two-dimensional beam with three degrees of freedom, as shown in Figure 3.

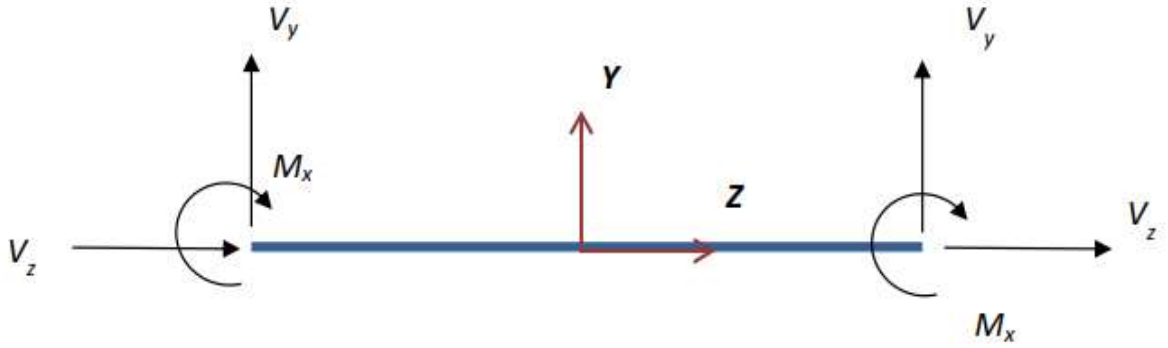

Figure 3- 2D beam element with 3 DOFs at each node.

$$\mathbf{K}_{g,i} = \frac{\mathbf{T}}{30\xi}\begin{bmatrix} 30 & 0 & 0 & -30 & 0 & 0 \\ 0 & 36 & 3\xi & 0 & -36 & 3\xi \\ 0 & 3\xi & 4\xi^2 & 0 & -3\xi & -\xi^2 \\ -30 & 0 & 0 & 30 & 0 & 0 \\ 0 & -36 & -3\xi & 0 & 36 & -3\xi \\ 0 & 3\xi & -\xi^2 & 0 & -3\xi & 4\xi^2 \end{bmatrix} \quad (5)$$

In the above matrix, **T** is the PF and ξ is the length of the element. Also, the local pseudo load at each node $\mathbf{P}_i^e$ can be correlated with $\mathbf{K}_{g,i}$ and nodal displacement $\{x\}_i$ as shown in Equation (6).

$$\mathbf{P}_i^e = [\mathbf{K}_{g,i}]\,\{x\}_i \quad (6)$$

As a result, it is possible to estimate the average PF by measuring displacements and rotations at each point of interest. This estimation is achieved by calculating the local pseudo load at each node within the selected element.

3. Improved PF and MF Identification via TLSF

LSF is an important concept in the Finite Element Method (FEM) that helps to accurately represent the force or load distribution on a structure. The use of LSFs also facilitates the use of higher-order elements, which can result in more accurate results than those obtained with lower-order elements. Since higher-order elements can represent complex load distributions more accurately, simulations of the structure's behaviour are more accurate.

As shown in Equation (3), to identify the unknown forces, LSF matrix is constructed as a block diagonal matrix using shape function column vectors. The arrangement of the block diagonal matrix of LSF is shown in Figure 4 (Reid & Jennings, 1984). It is possible to express the number of time steps within the element (ε) in terms of both the sampling frequency (f_s) and the main frequency of LSF (F_l). Using the power spectral density (PSD) variation of the measured response in relation to the structure's frequency, the main frequency can be determined. The time step between each node is assumed to be equal to half LSF period.

$$\varepsilon = \frac{f_s}{2F_l} \quad (7)$$

It is crucial that the frequency range of LSF matrix is higher than the primary frequency range of the unknown force that needs to be identified when creating LSF matrix. It is thus ensured that LSF matrix accurately captures the characteristics of the force and produces reliable results. To obtain the appropriate frequency F_l, PSD curve is developed by converting time-domain measurements into frequency-domain measurements using Fast Fourier Transform (FFT).

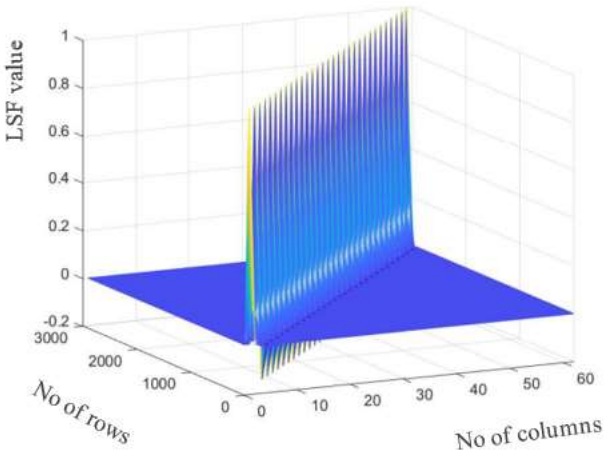

Figure 4 – Block diagonal matrix of LSF

To study the sensitivity of the F_l and its influence on force identification accuracy, a 6m span simply supported prestressed box girder bridge model with 2nos of 15.2mm parabolic tendons is used to apply different levels of PFs as shown in Figure 5 and Table 1. In this study, 170.0kN and 380.0kN PFs are applied with different vehicle excitation force to measure the vertical displacements and longitudinal strains at each node as tabulated in Table 2. The sampling frequency and sampling time are 1000Hz, 3s respectively.

A laboratory bridge model (Xiang et al., 2017) with a PF of 171.3kN is used in this study for the validation of the numerical model. The concrete density and elastic modulus used are 2.68×10^3 kg/m^3 and 28.66 GPa respectively. The different PFs are applied as external pseudo loads, a time-varying impulsive excitation force is applied at the midpoint of the beam as illustrated in Table 2, and dynamic responses are measured at the midpoint of the beam considering the worst-case scenario.

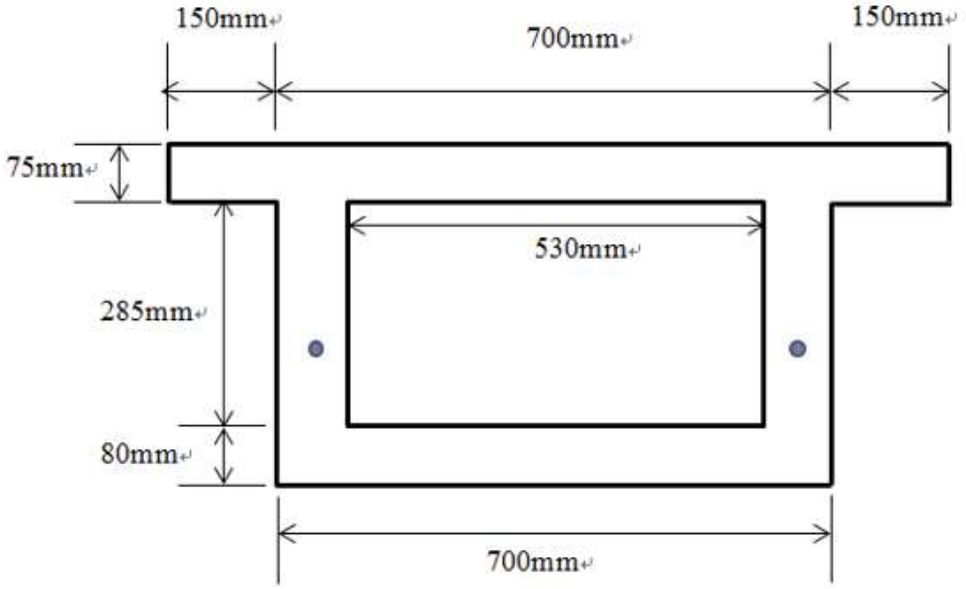

Figure 5- Geometry of the simply supported prestressed box girder bridge model.

Table 1- Parabolic tendon arrangement in the simply supported box girder.

Longitude (mm)	0	500	1000	1500	2000	2500	3000
Distance (mm)	235	209	184	163	146	134	130

Table 2- Vehicle excitation and PF for the numerical and laboratory model.

Cases	**PF /(kN)**	**Excitation force /(N)**
1	170.0	$20000(1 + 0.73Sin(10\pi(t - 0.02)))$
2	380.0	$20000(1 + 0.73Sin(10\pi(t - 0.02)))$
Laboratory model	171.3	$4985(1 + 0.73Sin(10\pi(t - 0.02)))$

ABAQUS software is used with C3D8R solid elements to model the box girder bridge. Displacement responses are compared with laboratory model responses and different noise levels, such as 2%, 5% and 10%, are added to the displacement responses obtained from the numerical study. The polluted dynamic responses (Y_i^P) for the synergic identification of PF and MF, estimated responses (Y_i^e) are generated by introducing random white noise in the following manner.

$$Y_i^p = Y_i^e\ (1 + \in_P . \emptyset_i) \tag{8}$$

where, $\in_P$ represents the level of noise and $\emptyset_i$ represents a random value obtained from a standard normal distribution. The deformed shape of the box-girder bridge model is shown in Figure 6.

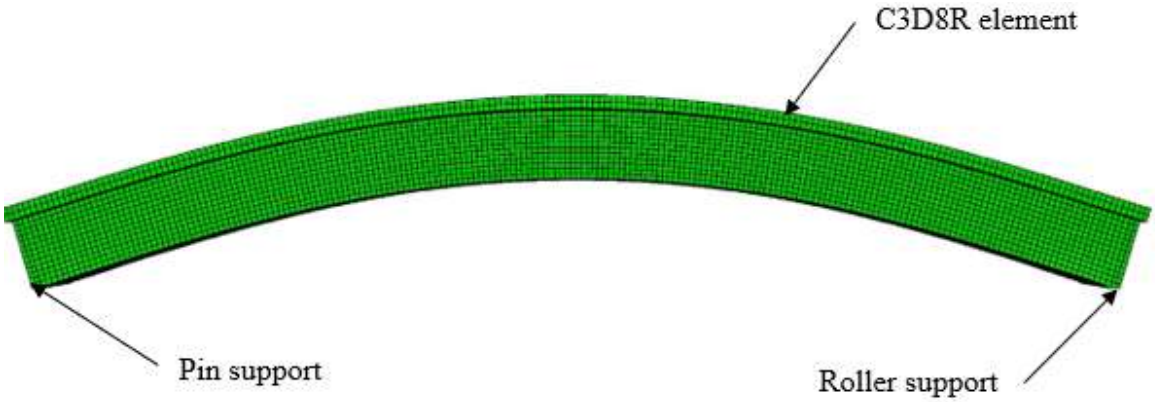

Figure 6- Deformed shape of the prestressed box girder bridge model.

A correlation exists between noise levels and LSF's main frequency, noting that an increase in noise levels can lead to a corresponding increase in LSF's main frequency. As a result, it emphasizes the sensitivity of frequency to noise levels, and the importance of implementing appropriate regularization methods to enhance force identification accuracy.

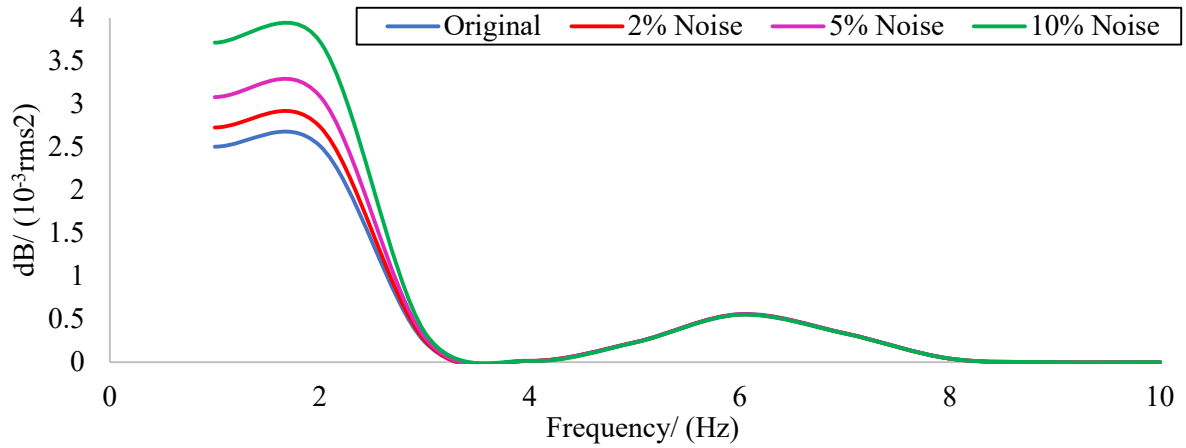

Figure 7- Power spectral density curve with different noise levels.

The analysis of PSD curve presented in Figure 7 reveals that the main frequency of the system increases as the noise levels rises. This observation strongly indicates that the main frequency is particularly sensitive to changes in noise levels. The impact of LSF frequency on the precision of PF and MF identification is evaluated through the computation of the condition number. This number represents the ratio of the maximum to minimum singular values of the bridge-vehicle system. Frequencies of 5Hz, 10Hz, and 20Hz are analysed for this purpose. The changes in singular values are illustrated in Figure 8, revealing a consistent decline as the LSF frequency rises. Correspondingly, the condition number diminishes with higher LSF frequencies. Consequently, the enhancement in LSF frequency contributes to a reduction in the inherent ambiguity of the prestressed bridge-vehicle system.

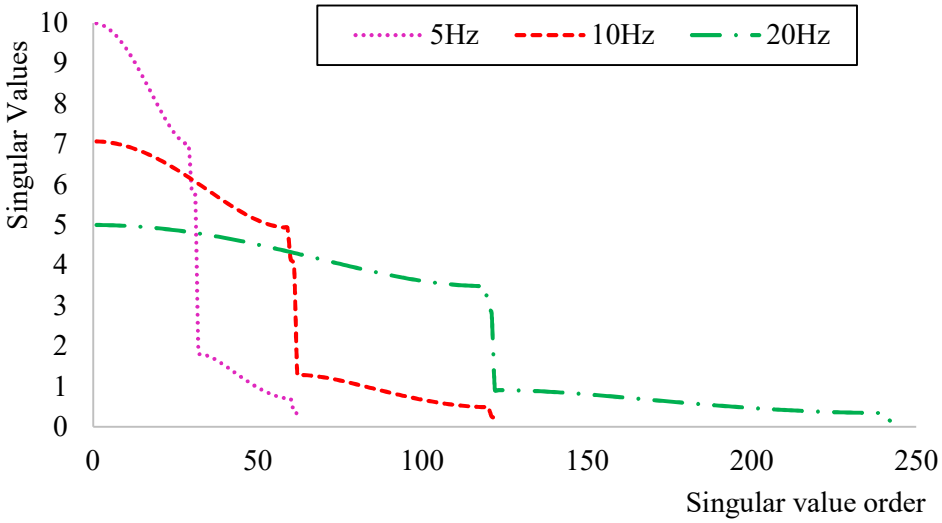

Figure 8- Influence of LSF's frequency on the singular values.

To propose a simplified approach for improving force identification accuracy by reducing the ill-posedness in LSF, an advanced technique involving a truncating coefficient (ψ) has been introduced. The approach is based on modifying the shape function of each node by incorporating the ψ value. This is accomplished by eliminating small elements from the matrix

corresponding to the shape function as shown in Equation 9. This modification improves the conditioning of the LSF problem and results in more accurate force identification.

$$\psi = \frac{\sum_{i=1}^{p} n_{N_{1,i}} + \sum_{\varepsilon-p}^{p} n_{N_{2,i}} + \sum_{\varepsilon-p}^{\varepsilon} n_{N_{3,i}} + \sum_{\varepsilon-p}^{p} n_{N_{4,i}}}{\sum_{i=1}^{\varepsilon} (n_{N_{1,i}} + n_{N_{2,i}} + n_{N_{3,i}} + n_{N_{4,i}})} \tag{9}$$

where, $n_{N_{1,i}}, n_{N_{2,i}}, n_{N_{3,i}}$ and $n_{N_{4,i}}$ represent the number of elements in the matrix relative to the shape function, while p is the truncating point on the column matrix of the shape function. In general, a value of ψ are within the range of 0.9 and 0.95. Consequently, the identification of unknown forces ($\mathbf{F}$) incorporating TLSFs can be expressed in the following manner along with the pertinent coefficient ($\boldsymbol{\alpha}$).

$$\mathbf{F} = \psi \mathbf{N} \boldsymbol{\alpha} \tag{10}$$

Analysing the shape function obtained by considering the frequency 5Hz, a ψ value of 0.925 is obtained, and accordingly PF and MF are compared as shown in Figure 9. The relative percentage error (RPE) can be obtained from the following relationship.

$$\text{RPE} = \frac{||\mathbf{F}_{\text{identified}} - \mathbf{F}_{\text{true}}||}{||\mathbf{F}_{\text{true}}||} \times 100\% \tag{11}$$

Based on TLSF, RPE has been reduced by 40.50% as compared to RPE obtained from LSF in MFI, while it has been reduced by 33.33% as compared to RPE obtained from LSF in PFI. The same improvement pattern is observed in numerical studies as well as laboratory studies. TLSF approach proposed in this study effectively addresses the issue of ill-posedness resulting from LSF. It is crucial to carefully select the truncation coefficient to improve the accuracy of identifying PF and MF synergistically.

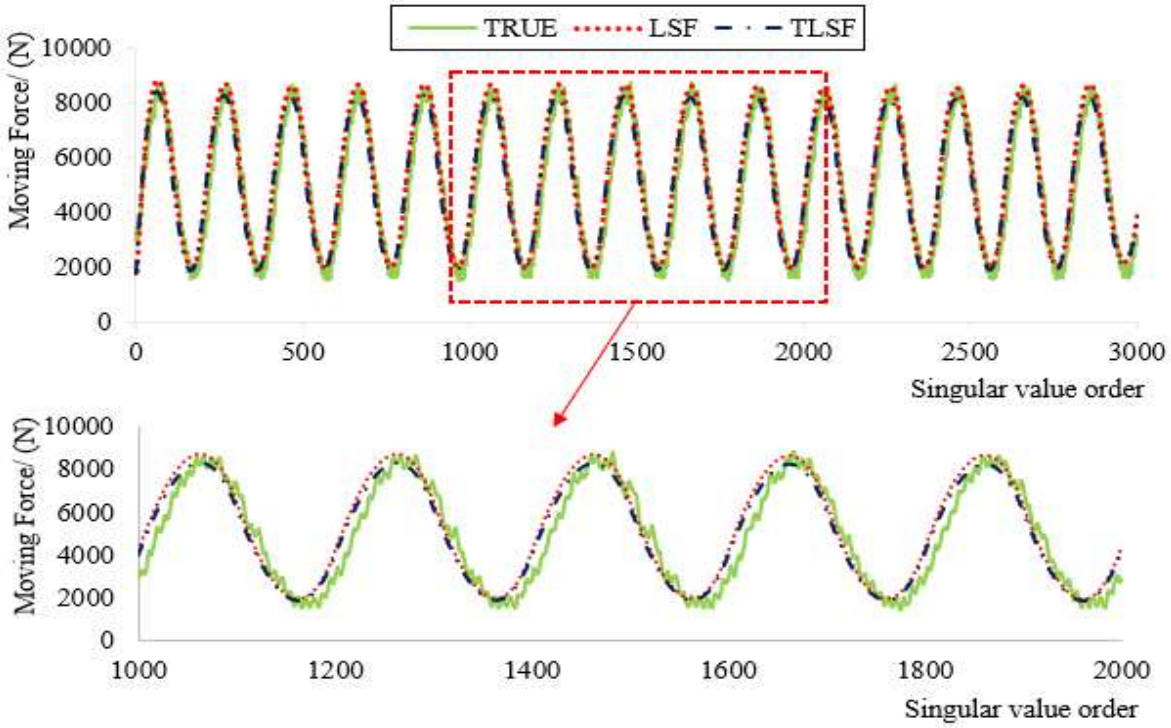

(a)

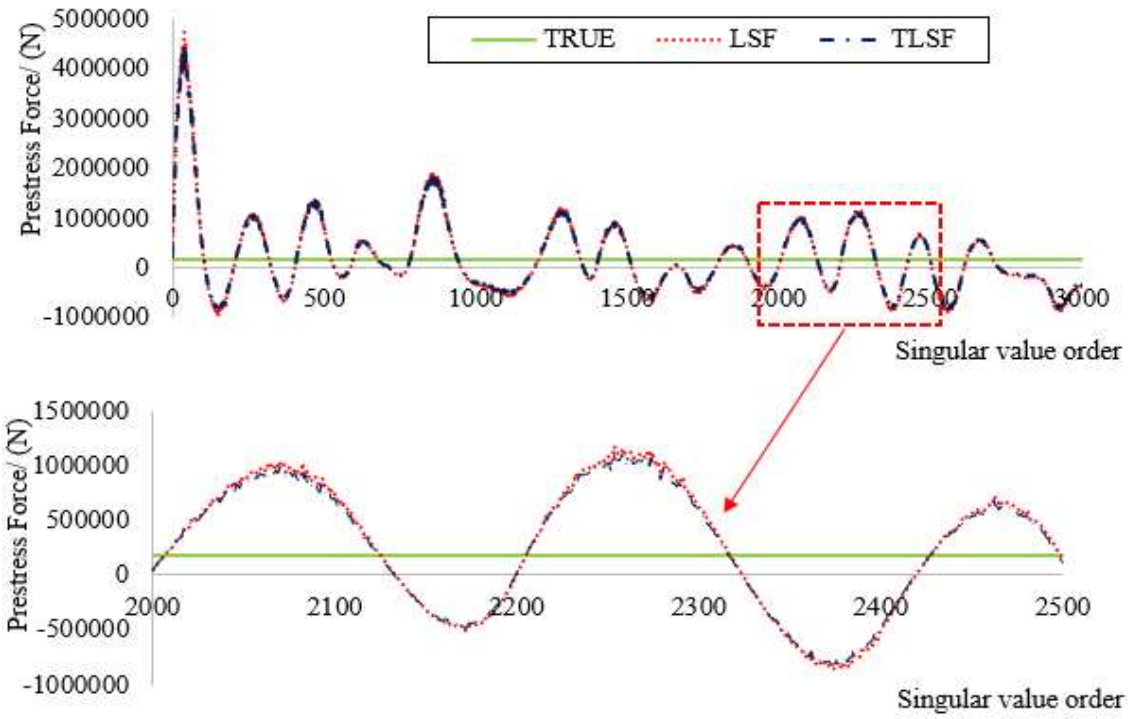

(b)

Figure 9- Force identification using laboratory data incorporated with LSF and TLSF: (a) MF (b) PF.

4. Conclusions

Ensuring the accurate synergic identification of PF and MF is of the utmost importance when estimating the in-service load carrying capacity of PCBs. This estimation involves considering the impact of existing PF, which is affected by both short-term and long-term losses, as well as MFs acting on the bridge structures. However, achieving accurate identification of PF and MF poses challenges due to the inverse problem's nature and the ill-conditioning caused by computational and observational errors. To address these challenges, this study introduces an improvement technique by incorporating a truncation coefficient into the LSF of the prestressed bridge-vehicle system. Through the proposed method, the following conclusions can be drawn, which contribute to enhanced accuracy and efficiency in PF and MF identification.

TLSF approach demonstrates its capability to improve the accuracy of PF and MF identification. Additionally, this method streamlines the reduction procedure of ill-posedness by considering the proposed truncating coefficient throughout the entire time history of nodes. The results highlight several advantages of the proposed TLSF method, including high accuracy, effectiveness, and reduced computational effort in regularization.

The findings of this study will significantly contribute towards estimating the existing PF and MF with minimal data for structural health monitoring of PCBs. As a result of these findings, it will be possible to conduct forensic engineering assessments which will aid in the enhancement of the longevity of the bridge structure, thereby ensuring the safety of the public.

5. Acknowledgments

This research is part of a Discovery Project funded by the Australian Research Council (ARC), "Next Generation Bridge Monitoring using Novel Synergic Identification" (DP220102045). The authors also would like to acknowledge Dr. Ziru Xiang for providing the experimental data and other assistance to conduct this research.

6. References

- Chan, T. H. T., Law, S. S., Yung, T. H., & Yuan, X. R. (1999). An interpretive method for moving force identification. *Journal of Sound and Vibration*, *219*(3), 503–524. https://doi.org/10.1006/jsvi.1998.1904
- Chan, T. H. T., Yu, L., Law, S. S., & Yung, T. H. (2001). Moving force identification studies, I: Theory. *Journal of Sound and Vibration*, *247*(1), 59–76. https://doi.org/10.1006/jsvi.2001.3630
- Chen, Z., & Chan, T. H. T. (2017). A truncated generalized singular value decomposition algorithm for moving force identification with ill-posed problems. *Journal of Sound and Vibration*, *401*, 297–310. https://doi.org/10.1016/j.jsv.2017.05.004
- Chen, Z., Chan, T. H. T., & Yu, L. (2020). Comparison of regularization methods for moving force identification with ill-posed problems. *Journal of Sound and Vibration*, *478*, 115349. https://doi.org/10.1016/j.jsv.2020.115349
- Gan, B.-Z., Chiew, S.-P., Lu, Y., & Fung, T.-C. (2019). The effect of prestressing force on natural frequencies of concrete beams – A numerical validation of existing experiments by modelling shrinkage crack closure. *Journal of Sound and Vibration*, *455*, 20–31. https://doi.org/10.1016/j.jsv.2019.04.030
- Gao, J., Shi, B., Zhang, W., & Zhu, H. (2006). Monitoring the stress of the post-tensioning cable using fiber optic distributed strain sensor. *Measurement*, *39*(5), 420–428. https://doi.org/10.1016/j.measurement.2005.12.002
- Reid, J. K., & Jennings, A. (1984). On Solving Almost Block Diagonal (Staircase) Linear Systems. *ACM Transactlons on Mathematical Software*, *10*(2), 196–201.
- Law, S. S., Chan, T. H. T., & Zeng, Q. H. (1997). Moving force identification: A time domain method. *Journal of Sound and Vibration*, *201*(1), 1–22. https://doi.org/10.1006/jsvi.1996.0774
- Law, S. S., Chan, T. H. T., & Zeng, Q. H. (1999). Moving Force Identification—A Frequency and Time Domains Analysis. *Journal of Dynamic Systems, Measurement, and Control*, *121*(3), 394–401. https://doi.org/10.1115/1.2802487
- Law, S. S., & Fang, Y. L. (2001). Moving force identification: optimal state estimation approach. *Journal of Sound and Vibration*, *239*(2), 233–254. https://doi.org/10.1006/jsvi.2000.3118
- Law, S. S., & Lu, Z. R. (2005). Time domain responses of a prestressed beam and prestress identification. *Journal of Sound and Vibration*, *288*(4–5), 1011–1025. https://doi.org/10.1016/j.jsv.2005.01.045
- Saiidi, M., Douglas, B., & Feng, S. (1994). Prestress Force Effect on Vibration Frequency of Concrete Bridges. *Journal of Structural Engineering*, *120*(7), 2233–2241. https://doi.org/10.1061/(ASCE)0733-9445(1994)120:7(2233)
- Xiang, Z., Chan, T. H. T., Thambiratnam, D. P., & Nguyen, T. (2017) Prestress and excitation force identification in a prestressed concrete box-girder bridge. *Computers and Concrete*, *20*, 617. doi: 10.12989/sss.2016.17.6.917.

- Xiang, Z., Chan, T. H. T., Thambiratnam, D. P., & Nguyen, T. (2016). Synergic identification of prestress force and moving load on prestressed concrete beam based on virtual distortion method. *Smart Structures and Systems*, *17*(6), 917–933. https://doi.org/10.12989/sss.2016.17.6.917
- Xuan, F.-Z., Tang, H., & Tu, S.-T. (2009). In situ monitoring on prestress losses in the reinforced structure with fiber-optic sensors. *Measurement*, *42*(1), 107–111. https://doi.org/10.1016/j.measurement.2008.04.011
- Yang, J., Hou, P., Yang, C., & Zhang, Y. (2021). Study on the Method of Moving Load Identification Based on Strain Influence Line. *Applied Sciences*, *11*(2), 853. https://doi.org/10.3390/app11020853
- Zhong, J., Xiang, Z., & Li, C. (2022). Synchronized Assessment of Bridge Structural Damage and Moving Force via Truncated Load Shape Function. *Applied Sciences*, *12*(2), 691. https://doi.org/10.3390/app12020691